

Tsunami sources in the southern California bight

José C. Borrero

Department of Civil and Environmental Engineering, University of Southern California, Los Angeles, California, USA

Mark R. Legg

Legg Geophysical, Huntington Beach, California, USA

Costas E. Synolakis

Department of Civil and Environmental Engineering, University of Southern California, Los Angeles, California, USA

Received 25 March 2004; revised 3 June 2004; accepted 8 June 2004; published 10 July 2004.

[1] Locally generated tsunamis due to faulting or slope failures offshore southern California threaten nearby coastal cities. Disruption of operations at port facilities due to tsunami attack could severely impact the regional and national economies. This study examines three faults and two landslides scenarios as potential tsunami sources. Computed runup ranges from 0.5 to 6 m depending on the source and location. Bathymetric features such as the broad San Pedro Shelf are shown to contribute to tsunami wave focusing while retarding tsunami arrival times, suggesting the usefulness of an early warning system. **INDEX TERMS:** 4564 Oceanography: Physical: Tsunamis and storm surges; 3099 Marine Geology and Geophysics: General or miscellaneous; 7212 Seismology: Earthquake ground motions and engineering; 7215 Seismology: Earthquake parameters; 7223 Seismology: Seismic hazard assessment and prediction. **Citation:** Borrero, J. C., M. R. Legg, and C. E. Synolakis (2004), Tsunami sources in the southern California bight, *Geophys. Res. Lett.*, 31, L13211, doi:10.1029/2004GL020078.

1. Introduction

[2] Historically, tsunamis have followed strong offshore earthquakes in California. These include events in the Santa Barbara Channel [1812], west of Point Conception [1927], and questionably, in Santa Monica Bay [1930]. Although there have not been any instrumental recordings of locally generated tsunamis in our study region, there have been anecdotal accounts of waves after locally strong earthquakes. Historical tsunami events are discussed in detail by McCulloch [1985] and Lander *et al.* [1993].

2. Regional Geologic Setting

[3] The Borderland offshore southern California consists of generally northwest-trending ridges, banks, and basins (Figure 1). This ridge and basin structure persists as the San Andreas fault system accommodates about 52 ± 2 mm/yr of right shear between the Pacific and North America tectonic plates. As much as 20% (10–11 mm/yr) of the relative motion occurs on offshore faults [DeMets and Dixon, 1999]. Vertical deformation occurring along coastal and offshore fault zones is directly responsible for uplift of coastal and island marine terraces [Lajoie *et al.*, 1992].

[4] Like the San Andreas Fault, strike-slip faults offshore southern California have sinuous traces with restraining and releasing bends. Tectonic events at these bends create both seafloor uplift and subsidence, which could in turn generate tsunamis [Legg and Kennedy, 1991]. The high-relief Borderland seafloor consists of many steep slopes underlain by fractured and deformed bedrock and covered by slide prone sediments [Schwab *et al.*, 1993]. Legg and Kamerling [2002] report evidence of large basement-involved landslides in the Borderland. Major submarine landslides in sedimentary rocks along the over steepened slopes offshore Palos Verdes Peninsula (PVP) have also been reported [Bohannon and Gardner, 2004]. This combination of active faulting and landsliding makes the Borderland rich in potential tsunami sources.

2.1. Tectonic Tsunami Sources

[5] For this study, we consider three tectonic sources. The Catalina Fault (CAT) and the island uplift, the Lasuen Knoll (LAS) along the southern Palos Verdes Fault, and the San Mateo Thrust Fault (SAM) in southern Orange County (see Figures 1 and 2). The first two represent restraining bends along major strike-slip faults; the latter is a low-angle thrust fault with significant right-lateral slip.

[6] As noted by Geist [2002], complex rupture processes have important effects on tsunami generation and local runup. Real earthquakes have non-uniform slip distributions [Wald and Heaton, 1994]. We thus develop multiple segment fault rupture and earthquake source models that use several segments with different fault geometries and slip vectors.

[7] Fault strike and segment geometry (see Table 1) is derived from offshore fault mapping based on seismic reflection profiling and seafloor morphology [Greene and Kennedy, 1987]. Fault dip and down-dip width are poorly constrained for many offshore faults including those along the Catalina Escarpment. Due to the overall strike-slip character of major northwest-trending offshore fault zones, the fault dip is expected to be near vertical. Seismic reflection profiles provide control on fault dips for the low-angle San Mateo Thrust [MMS, 1997]. The down dip width is consistent with seismogenic depth observed throughout southern California. The modeled dips and widths of the restraining bend fault segments are consistent with those inferred for the Palos Verdes Hills Fault [Ward and Valensise, 1994] and for the 1989 Loma Prieta earthquake [Marshall *et al.*, 1991].

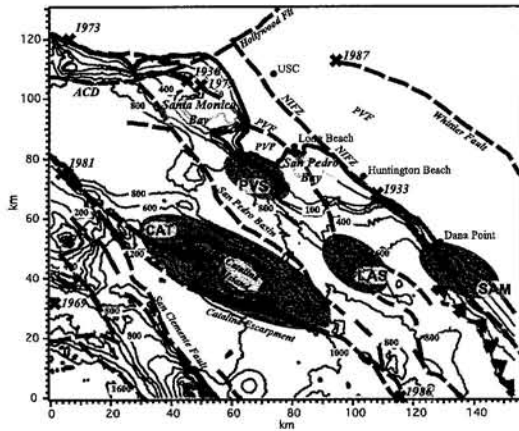


Figure 1. A map of the central Southern California Bight showing offshore bathymetry, major offshore faults (dashed traces), significant historical earthquakes (black x's) and regions considered for tsunami generation (grey ovals).

[8] To calibrate possible earthquake and faulting parameters, we attempt to match the shape of the long-term seafloor uplift observed at Santa Catalina Island, Lasuen Knoll, and San Mateo Thrust [Legg *et al.*, 2004]. The fault displacements used for the earthquake source are scaled to represent realistic displacements observed in other large earthquakes throughout California and the world [Wells and Coppersmith, 1994].

2.2. Submarine Landslide Tsunami Sources

[9] We consider one submarine landslide source on the Palos Verdes Escarpment, southwest of the PVP. Landslide scars and deposits have been observed and described in this region since the 1950's [McCulloch, 1985]. One feature in particular, dubbed the Palos Verdes Debris Avalanche or the Palos Verdes Slide (PVS) is believed to be the signature of a tsunamigenic submarine landslide. Bohannon and Gardner [2004] used bathymetric data and seismic reflection profiles to map the scar and debris field. They estimated that the slide displaced between 0.3 and 0.7 km³ of material which covers 32 km² of the seafloor. Normark *et al.* [2004] use radiocarbon dating to estimate the age of deposits from the PVS at 7500 years. Locat *et al.* [2004] analyzed the slope stability and deposition patterns of the debris field and conclude that the PVS occurred as a catastrophic single event that was likely triggered by a $M \approx 7$ local earthquake.

[10] Both Bohannon and Gardner [2004] and Locat *et al.* [2004] state that the PVS was capable of generating a substantial tsunami and estimate initial waves ranging from 8 to 50 m. Since the geometry and volume of the landslide have been well constrained, the variability reflects uncertainties in geomechanical properties and hydro-generation characteristics.

3. Tsunami Modeling

[11] Tsunami modeling involves three computational phases: generation, propagation, and runup [Liu *et al.*, 1991]. For tectonic tsunamis, the initial condition is obtained directly from the expected coseismic vertical deformation per Okada's [1985] method. For landslide

sources, the predicted surface displacement at the end of wave generation may be used as the initial condition.

[12] We use a mid-range value for the total tsunami amplitude from the analysis of Bohannon and Gardner [2004]. The wave shape is then based on empirical relationships described in Raichlen and Synolakis [2003] and Synolakis [2003]. For each case, we use an asymmetric dipole shape with a Gaussian profile and a hyperbolic secant profile for the transverse direction. The drawdown is assumed to be 70% of the total amplitude and the positive wave is 30%. Additional landslide wave generation models are discussed in Borrero [2002] and Synolakis [2003].

[13] Initial condition PVS1 is located directly over and scaled to the existing scar described by Bohannon and Gardner [2004]. To investigate the effect of source location, we positioned an identical wave shape, PVS2, at the

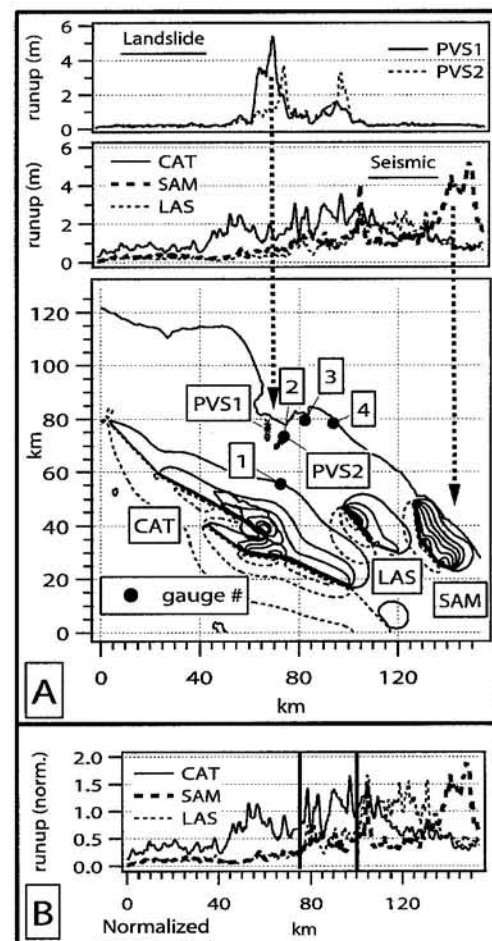


Figure 2. Panel A: Runup plots for each of the five scenarios. Computed runup along the south facing shoreline is depicted on the upper graphs. Contour plots show initial condition of the tsunami simulation, solid for uplift, dashed for subsidence. The values of maximum positive and negative initial values are given in Table 2). Contour intervals are 40 cm for each tectonic case. Wave gauge locations are indicated with black dots and numbered boxes. Panel B: Runup normalized by maximum coseismic uplift for the three tectonic scenarios. The region between the black vertical lines is the Ports region in San Pedro Bay.

Table 1. Earthquake Source Parameters for Tsunami Simulations^a

Fault	Seg.	L W		Dip	Strike	Disp. Dep. ^c		
		(km)	(km)			(m)	(km)	
Santa Catalina $M_w = 7.6$	1	21.9	14.0	89	173	313	4.0	0.5
	2	28.2	14.0	85	143	293	5.0	1.0
	3	16.1	14.0	70	124	277	4.8	1.0
	4	20.2	14.0	80	146	303	3.6	1.0
	5	8.0	14.0	80	149	300	6.4	1.5
	6	40.2	14.0	80	153	297	4.5	1.0
	7	29.7	14.0	89	166	315	4.1	0.5
Lasuen Knoll $M_w = 7.1$	1	8.8	12.8	70	135	290	1.5	0.5
	2	7.9	12.2	80	135	318	3.0	0.5
	3	10.0	12.2	80	135	316	5.0	0.5
San Mateo Thrust $M_w = 7.0$	1	5.5	12.0	45	120	293	4.0	0.5
	2	11.4	12.0	45	120	322	4.0	0.5
	3	15.0	12.0	45	120	350	4.0	0.5

^aRake of slip vector measured from downdip direction, rightslip = 180 deg.

^bDepth to top of fault plane below top of elastic half space.

southern end of and perpendicular to the San Pedro Escarpment, allowing for the direct comparison of two scenarios.

[14] Similar asymmetric dipole shapes were used to successfully model the 1998 Papua New Guinea event [Synolakis *et al.*, 2002]. The results also compared favorably with Boussinesq type models in terms of leading wave amplitude, leading wave arrival time and runup at the shoreline [Lynett *et al.*, 2003].

[15] For tsunami propagation and runup, we use the model "MOST" [Titov and González, 1997]. MOST uses the non-linear, shallow water wave equations to simulate the propagation of long waves over an arbitrary bathymetry. For runup, the model uses a moving boundary algorithm, which propagates the wave front on to the dry topography [Titov and Synolakis, 1998]. We used a 150-m numerical grid with a time step of 1 second, simulations were carried out for 3000 seconds. The 150-m computational grid is adequate for determining regional runup distributions, but may not be of sufficient resolution for detailed inundation modeling as routinely performed by MOST.

4. Discussion

[16] We computed runup for each scenario along the south and west facing shorelines while time series of water surface elevations were recorded at selected locations. Figure 2 shows a steep narrow runup distribution for the landslide sources and a broad distribution for the tectonic cases (Figure 2, panels A & B). The highest runup is computed at 5.5 m for the PVS1 case, however this runup occurs on the steep cliffs of the Palos Verdes Peninsula. For both PVS cases, a region of elevated runup is observed at the eastern end of San Pedro Bay, near the entrance to Anaheim Bay.

[17] The tectonic cases (Figure 2, Panel A) predict runup between 0.5 m and 5.0 m. The largest runup values occur for the San Mateo Thrust case on shorelines adjacent to the region of coseismic deformation. Uncertainty due to factors such as heterogeneous fault slip and more complex fault geometry could lead to significantly higher values for localized runup [Geist, 2002].

4.1. Tsunami Focusing and Amplification

[18] To identify coastal regions susceptible to tsunami wave amplification, the runup from each earthquake sce-

Table 2. Range of Maximum Values for Each Initial Condition

Case	Positive	Negative
Catalina 1	+2.17 ^a m	-1.17 m
San Mateo	+2.43 m	-0.32 m
Lasuen Knoll	+1.74 m	-1.20 m
PV Slide 1	+3.00 m	-7.00 m
PV Slide 2	+3.00 m	-7.00 m

^aThis value occurred over land and did not contribute to wave generation.

nario was normalized by the maximum coseismic uplift for each case. Table 2 gives the values used for the normalization. The results are shown in Figure 2, Panel B. we find maximum runup within 50% and 150% of initial wave heights. Regions of the coast where the normalized runup is greater than 1.0 amplify tsunami waves. This is evident for the CAT where the shallow bathymetry of the San Pedro Shelf leads to wave focusing and larger runup around the Ports [Legg *et al.*, 2004]. Previous tsunami hazard studies for distant sources along the southern California coast [Houston, 1980; McCulloch, 1985] show similar patterns of amplification in Santa Monica Bay and San Pedro Bay.

[19] The normalized runup for the CAT case (Figure 2, Panel C) may under-represent the amplification, because the largest value for coseismic uplift used to normalize the runup data occurred on land (over Catalina Island) and did not contribute directly to the initial wave. We used the maximum uplift in an attempt to be consistent with the other cases. Use of a smaller value for the normalization of the CAT runup suggests that even more widespread areas may experience amplification of tsunami waves.

[20] In addition, we consider the possibility of a tsunami-genic landslide initiated by a local earthquake. Locat *et al.* [2004] suggest that a magnitude $\cong 7$ earthquake may have triggered the PVS. In such a case, the coastline might then experience the additive effects of two tsunami sources, as well as possible wave interactions, not considered in this study.

4.2. Arrival Times

[21] Figure 3 shows the relative arrival times of tsunami waves at the Ports of Los Angeles and Long Beach (LALB)

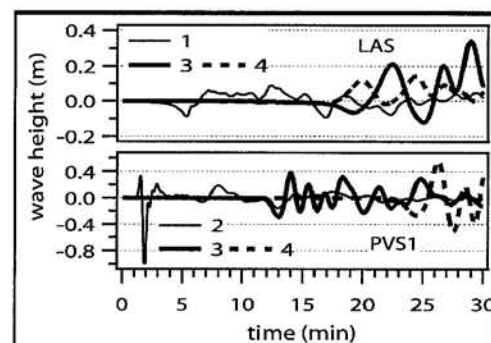


Figure 3. Time series of simulated tsunami waveforms at locations indicated in Figure 2. The upper plot shows the delay in tsunami arrival from the Lasuen Knoll (LAS) case between the deepwater gauge (#1) and port facilities in San Pedro Bay (gauges 3 and 4). The lower panel shows the delay in first wave arrival from the PVS1 case between gauge #2 (San Pedro Shelf) and the port gauges (3, 4).

relative to deepwater locations. Waves from the LAS scenario affect the deep water gauge within five minutes of tsunami generation, however the wave does not reach the harbor areas until 15 (Anaheim Bay) or 20 (LALB) minutes after generation. For the landslide cases (Figure 3, lower panel), we compute a delay of 12 minutes to the Ports of Los Angeles and Long Beach and a delay of 23 minutes to Anaheim Bay. Such an amount of time, coupled with increased tsunami awareness and proper procedures, could make a local tsunami warning effective and allow for the cessation of hazardous port operations and a safe evacuation of personnel.

5. Conclusions

[22] We modeled the coastal runup for both tectonic and landslide generated tsunami sources offshore of Southern California. Tsunami sources were based upon the best available geologic information. Runup heights ranged from 0.5 to 6 m along the coast depending on the type, size and location of the source. Landslide tsunamis produced extreme runup peaks with a narrow alongshore distribution, while tectonic sources produced broader, more regional effects. This is similar to run up distributions observed after actual tsunamis [Borrero et al., 2003] and results obtained in other modeling efforts [Borrero et al., 2001; Okal and Synolakis, 2004]. Amplification effects were observed along the south facing shores of San Pedro Bay, home to two important container ports and a Navy base. The shallow bathymetry that focuses and amplifies waves into this region also slows their arrival by as much as 20 minutes compared to deepwater locations. This significant delay may allow for an effective local tsunami warning system for the Ports of Los Angeles, Long Beach and Anaheim Bay.

[23] **Acknowledgments.** We acknowledge the EERI/FEMA NEHRP Fellowship awarded to Dr. Legg, as well as support from the California State Office of Emergency Services and the National Science Foundation. Angie Venturato of NOAA/PMEL provided combined bathymetry and topography grids for the model. We also thank the two anonymous reviewers for their valuable comments.

References

- Bohannon, R., and J. Gardner (2004), Submarine landslides of San Pedro Escarpment, *Mar. Geol.*, **203**, 261–268.
- Borrero, J. C. (2002), Tsunami hazards in southern California, Ph.D. thesis, Univ. of S. Calif., Los Angeles.
- Borrero, J. C., J. F. Dolan, and C. E. Synolakis (2001), Tsunamis within the eastern Santa Barbara Channel, *Geophys. Res. Lett.*, **28**, 643–646.
- Borrero, J., J. Bu, C. Saiang et al. (2003), Field survey and preliminary modeling of the Wewak Papua New Guinea tsunami, *Seismol. Res. Lett.*, **74**, 393–405.
- DeMets, C., and T. H. Dixon (1999), New kinematic models for Pacific–North America motion from 3 Ma to present: I. Evidence for steady motion and biases in the NUVEL-1A model, *Geophys. Res. Lett.*, **26**, 1921–1924.
- Geist, E. L. (2002), Complex earthquake rupture and local tsunamis, *J. Geophys. Res.*, **107**(B5), 2086, doi:10.1029/2000JB000139.
- Greene, H. G., and M. P. Kennedy (1987), Explanation of the California continental margin map series, *Bull.* **207**, 110 pp., Calif. Div. of Mines and Geol., Sacramento.
- Houston, J. R. (1980), Type 19 flood insurance study: Tsunami predictions for southern California, *Tech. Rep. HL-80-18*, 172 pp., Corps of Eng. Waterw. Exp. Stn., Vicksburg, Miss.
- Lajoie, K. R., D. J. Ponti, C. L. Powell II et al. (1992), Quaternary sea-level fluctuations, in *Annual Field Trip Guidebook*, edited by E. G. Heath and W. L. Lewis, pp. 81–104, S. Coast Geol. Soc., Santa Ana, Calif.
- Lander, J. F., P. A. Lockridge, and M. J. Kozuch (1993), Tsunamis affecting the West Coast of the United States, 1806–1992, *KGRD* **29**, 242 pp., Natl. Oceanic and Atmos. Admin., Boulder, Colo.
- Legg, M. R., and M. J. Kamerling (2002), Large-scale basement-involved landslides, California Continental Borderland, *Pure Appl. Geophys.*, **160**, 2033–2051.
- Legg, M. R., and M. P. Kennedy (1991), Oblique divergence and convergence in the California Continental Borderland, in *Environmental Perils of the San Diego Region*, pp. 1–16, San Diego Assoc. of Geol., Calif.
- Legg, M., C. Synolakis, and J. Borrero (2004), Tsunami hazards associated with the Catalina Fault in southern California, *EERI Spectra*, **20**(3), 1–34.
- Liu, P. L.-F., C. E. Synolakis, and H. Yeh (1991), Impressions from the First International Workshop on Long Wave Runup, *J. Fluid Mech.*, **229**, 675–688.
- Locat, J., H. Lee, P. Locat, and J. Imran (2004), Numerical analysis of the mobility of the Palos Verdes debris avalanche, California, *Mar. Geol.*, **203**, 269–280.
- Lynett, P., J. Borrero, P. Liu, and C. Synolakis (2003), Field survey and numerical simulations: A review of the 1998 Papua New Guinea tsunami, *Pure Appl. Geophys.*, **160**, 2119–2146.
- Marshall, G. A., R. S. Stein, and W. Thatcher (1991), Faulting geometry and slip from coseismic elevation changes: The 18 October 1989, Loma Prieta, California, earthquake, *Bull. Seismol. Soc. Am.*, **81**, 1660–1693.
- McCulloch, D. S. (1985), Evaluating tsunami potential, in *Evaluating Earthquake Hazards in the Los Angeles Region—An Earth Science Perspective*, U.S. Geol. Surv. Prof. Pap., **1360**, 375–413.
- Minerals Management Service (MMS) (1997), Oceanside seismic data set, *POCS CD97-01*, U.S. Dep. of the Int., Washington, D. C.
- Normark, W., M. McGann, and R. Sliter (2004), Age of Palos Verdes submarine debris avalanche, southern California, *Mar. Geol.*, **203**, 247–259.
- Okada, Y. (1985), Surface deformation due to shear and tensile faults in a half-space, *Bull. Seismol. Soc. Am.*, **75**, 1135–1154.
- Okal, E. A., and C. Synolakis (2004), Source discriminants for near-field tsunamis, *Geophys. J. Int.*, in press.
- Raichlen, F., and C. E. Synolakis (2003), Runup from three dimensional sliding mass, in *Long Waves Symposium*, edited by M. Briggs and C. Koutitas, pp. 247–256, Thessaloniki, Greece, August 25–27.
- Schwab, W. C., H. J. Lee, and D. C. Twichell (1993), Submarine landslides: Selected studies in the U.S. Exclusive Economic Zone, *U.S. Geol. Surv. Bull.*, **2002**, 204 pp.
- Synolakis, C. E. (2003), Tsunami and seiche, in *Earthquake Engineering Handbook*, edited by W.-F. Chen and C. Scawthorn, pp. 1–90, CRC Press, Boca Raton, Fla.
- Synolakis, C. E., J.-P. Bardet, J. C. Borrero et al. (2002), The slump origin of the 1998 Papua New Guinea tsunami, *Proc. R. Soc. London, Ser. A*, **458**, 763–789.
- Titov, V., and F. González (1997), Implementation and testing of the Method Of Splitting Tsunami model, *NOAA Tech. Memo., ERL PMEL-112*, 11 pp.
- Titov, V., and C. E. Synolakis (1998), Modeling of tidal wave runup, *J. Waterw. Port Ocean Coastal Eng.*, **124**, 157–171.
- Wald, D. J., and T. H. Heaton (1994), Spatial and temporal distribution of slip for the 1992 Landers, California, earthquake, *Bull. Seismol. Soc. Am.*, **84**, 668–691.
- Ward, S. N., and G. Valensise (1994), The Palos Verdes terraces, California: Bathub rings from a buried reverse fault, *J. Geophys. Res.*, **99**, 4485–4494.
- Wells, D., and K. Coppersmith (1994), New empirical relationships among magnitude, rupture length, rupture width, rupture area, and surface displacement, *Bull. Seismol. Soc. Am.*, **84**, 974–1002.

J. C. Borrero and C. E. Synolakis, Department of Civil Engineering, University of Southern California, Los Angeles, CA 90089-2531, USA. (jborrero@usc.edu; costas@usc.edu)

M. R. Legg, Legg Geophysical, 16541 Gothard Street, Suite 107, Huntington Beach, CA 92647, USA. (mrlegg@attglobal.net)